Proceedings of the 16th Czech and Slovak Conference on Magnetism, Košice, Slovakia, June 13–17, 2016

Investigations of the Magnetization Reversal Processes in Nanocrystalline Nd–Fe–B Alloys Doped by Nb

M. Kaźmierczak, P. Pawlik, J.J. Wysłocki, I. Wnuk*, P. Gębara, K. Pawlik and A. Przybył

Institute of Physics, Częstochowa University of Technology, al. Armii Krajowej 19, 42-200 Częstochowa, Poland

In the following article the magnetic properties and phase composition of $(Nd_{10}Fe_{67}B_{23})_{100-x}Nb_x$ (where $x = 5, 6, 7, 8, 9$) alloys in the form of ribbons are discussed. The X-ray diffraction studies revealed the coexistence of amorphous and nanocrystalline structures consisting of $Nd_2Fe_{14}B$, $Nd_{1+\varepsilon}Fe_4B_4$ and metastable $Nd_2Fe_{23}B_3$ phases. The shape of M_{rev} (M_{irr}) suggests that the magnetization reversal proceeds through the nucleation of the reversal domain for the ribbon doped with 5–7 at.% of Nb and the subsequent pinning of the domain walls for ribbons doped with 8 and 9 at.% of Nb.

DOI: 10.12693/APhysPolA.131.789

PACS/topics: 75.30.Sg, 75.50.Bb

1. Introduction

For hard magnetic materials the magnetization reversal process can be studied by the analysis of minor hysteresis loops and recoil curves [1, 2]. In some nanocrystalline alloys a collective mechanism is possible [3–5], in which both pinning [6] and nucleation [7] processes can contribute to the magnetization reversal. In magnets where significant grain size distribution are encountered and an amorphous phase is present, nucleation H_N and pinning H_P field distributions are expected. The distribution of H_N and H_P values can considerably affect the M_{rev} vs. M_{irr} relationship. Furthermore, the microstructure and magnetic properties of nanocrystalline alloys have significant influence on the shape of the initial magnetization curve $J_r(H)$ as well as on the coercivity field vs. the maximum external magnetic field ${}_JH_c(H)$ curve. This problem is not widely studied in nanocrystalline melt-spun ribbon samples. In this case, the M_{rev} vs. M_{irr} relationship and ${}_JH_c(H)$ curve were used to study the differences in magnetic properties in the annealed $(Nd_{10}Fe_{67}B_{23})_{100-x}Nd_x$ (where $x = 5, 6, 7, 8, 9$) ribbons.

2. Sample preparation and experimental method

Alloy ingots of the nominal composition $(Nd_{10}Fe_{67}B_{23})_{100-x}Nb_x$ (where $x = 5, 6, 7, 8, 9$) were prepared from high purity constituent elements by arc melting in a Ti-gettered Ar atmosphere. Subsequently the ribbon samples were prepared by using a melt spinning technique in an Ar protective atmosphere. The linear speed of the copper roll surface of 35 m/s was used in the process. Samples were sealed-off in quartz tubes under a low Ar atmosphere. In order to obtain a nanocrystalline microstructure, the samples were annealed at a temperature ranging from 923 K to 1063 K for 5 min and cooled in water. The phase structure was determined from the analysis of the diffraction patterns. Hysteresis loops were measured using the LakeShore 7307 vibrating sample magnetometer at an external magnetic field of up to 2 T at room temperature. The M_{rev} vs. M_{irr} dependences were determined from the recoil curves measured at room temperature in the initially saturated samples as described in [8]. Furthermore, the field dependences of the coercivity and initial magnetization curves were obtained from the minor hysteresis loops.

3. Results and discussion

The X-ray diffraction (XRD) patterns measured for the $(Nd_{10}Fe_{67}B_{23})_{100-x}Nb_x$ (where $x = 5, 6, 7, 8, 9$) alloy ribbons in an as-cast state and those subjected to annealing at 923, 943, 1023, 1043, and 1063 K temperatures for 5 min, are shown in Fig. 1. For the as-cast ribbon samples, the amorphous halo showed visible broad peaks that corresponded to the crystalline phases which confirmed a partially crystalline structure. The low intensity of these peaks in comparison with the background measurements does not permit a clear identification of the crystalline phases present in the sample. The short time annealing of 5 min at 923 K and above temperatures resulted in significant changes in the crystalline structure of the material and led to the nucleation and growth of the crystalline phases. The crystalline phases observed in the annealed ribbons were as follows: the hard magnetic $Nd_2Fe_{14}B$, the paramagnetic $Nd_{1+\varepsilon}Fe_4B_4$ and the soft magnetic metastable $Nd_2Fe_{23}B_3$. The XRD pattern measured for the $(Nd_{10}Fe_{67}B_{23})_{100-x}Nb_x$ (where $x = 5$) alloy ribbons annealed at 1063 K for 5 min, are shown in Fig. 1b. For this composition the presence of reflexes coming from the soft magnetic α-Fe phase was confirmed. For higher annealing temperatures (above 963 K) hard magnetic properties were induced. The maximum values of the coercive ${}_JH_c = 1175$ kA/m was obtained for a

*corresponding author; e-mail: wnukiza@gmail.com

sample doped with 8 at.% of Nb and annealed at 1023 K. However, the heat treatment at 1003 K exhibited the maximum values of polarization remanence $J_r = 0.35$ T and the maximum energy product $(BH)_{\max} = 21$ kJ/m^3.

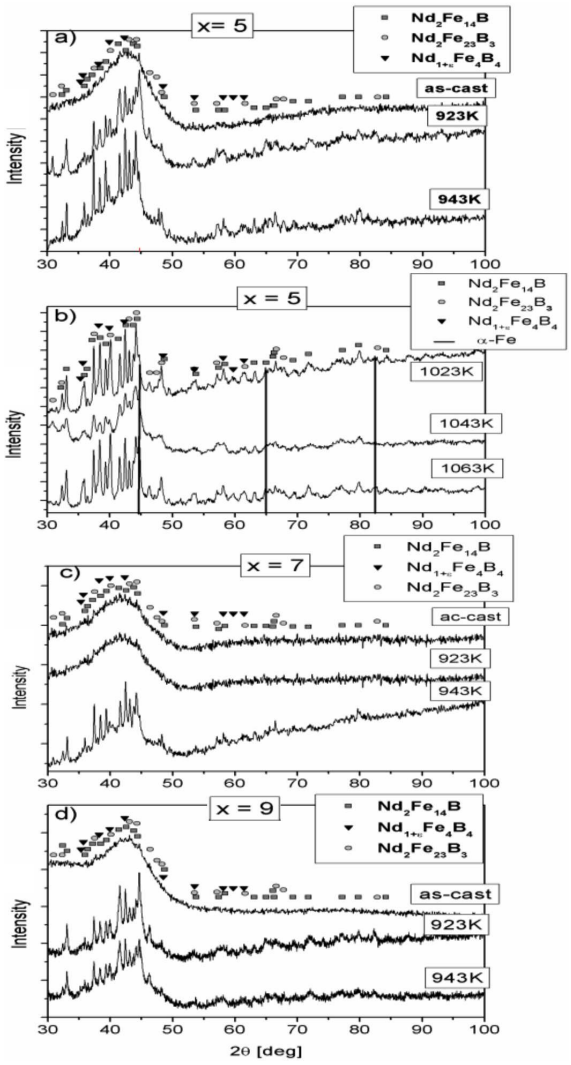

Fig. 1. X-ray diffraction patterns measured for $(Nd_{10}Fe_{67}B_{23})_{100-x}Nb_x$ (where $x = 5$ (a), $x = 5$ (b), $x = 7$ (c), $x = 9$ (d)) alloy as-cast and annealed ribbons.

The hysteresis loops of the selected ribbons are shown in Fig. 2. Due to their phase constituents and magnetic properties the studied samples seem to be good candidates for the investigation of the magnetization reversal process.

The M_{rev} vs. M_{irr} dependences for various H are shown in Fig. 3. Some differences between the behavior of the ribbons doped with Nb indicate substantial differences in the magnetization reversal processes. For the ribbon doped with 5–7 at.% of Nb the linear decrease of M_{rev} with the increase of M_{irr} suggests that the mean value of the nucleation field H_N distribution is higher than that of the pinning field H_P. For ribbons doped with 8 and 9 at.% of Nb the M_{rev} vs. M_{irr} revealed a shallow

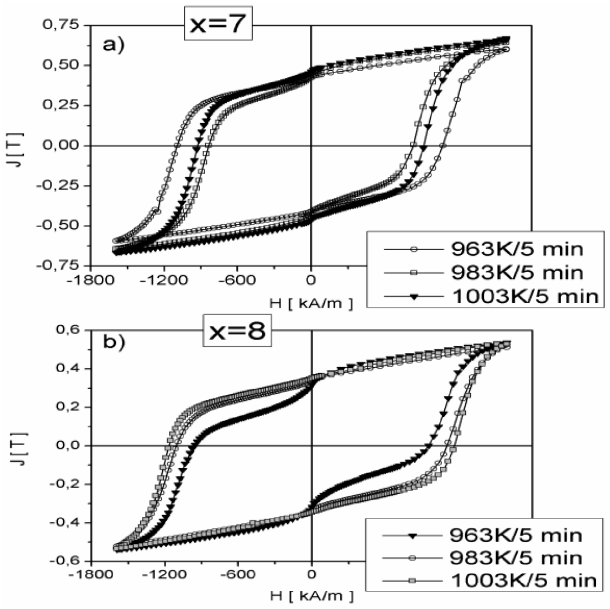

Fig. 2. The hysteresis loops measured for the $(Nd_{10}Fe_{67}B_{23})_{100-x}Nb_x$ (where $x = 7$ (a), $x = 8$ (b)) alloy ribbons samples annealed at 963–1003 K for 5 min.

minimum value corresponding to positive values of irreversible magnetization in low external magnetic fields. In such a system, pinning field H_P prevails in the nucleation field H_N or are very close to each other. Furthermore, shifts in the depths of the curves toward the positive values of M_{irr} suggest that the nucleated domain walls are swiftly pinned after nucleation.

Interesting information about the magnetization reversal process can be obtained for ribbons initially in the demagnetized state measured in low external magnetic fields. Dependences of the coercive ${}_JH_c$ in the maximum applied magnetic field H and initial magnetic polarization $J(H)$ curves are shown in Fig. 4. The studies were performed on a sample containing 8 at.% Nb revealing the best magnetic properties in the studied group of alloys. It was shown that the annealing temperature also has a significant impact on the shapes of the ${}_JH_c(H)$ and $J(H)$ curves. In the case of the ribbons annealed at 943 K, coercivity of ${}_JH_c$ and the initial polarization J increase almost linearly with the increase of the maximum applied magnetic field H. Different shapes of ${}_JH_C(H)$ and $J(H)$ curves were obtained for ribbons annealed at temperatures ranging from 963 to 1003 K. At lower applied fields up to 1000 kA/m, ${}_JH_C$ slightly increases to 104 kA/m and 39 kA/m, respectively for ribbons annealed at 963 K and 1003 K. At an applied magnetic field higher than $H = 800$ kA/m, a steep increase of the coercivity was observed (${}_JH_C = 941$ kA/m for 963 K and ${}_JH_C = 1151$ kA/m for 1003 K). Similar tendencies in the $J(H)$ curves were measured for the studied samples. Such shapes of the ${}_JH_c(H)$ and $J(H)$ curves for ribbons annealed at 963 K and 1003 K are typical for magnets where pinning of reversed domains is a domina-

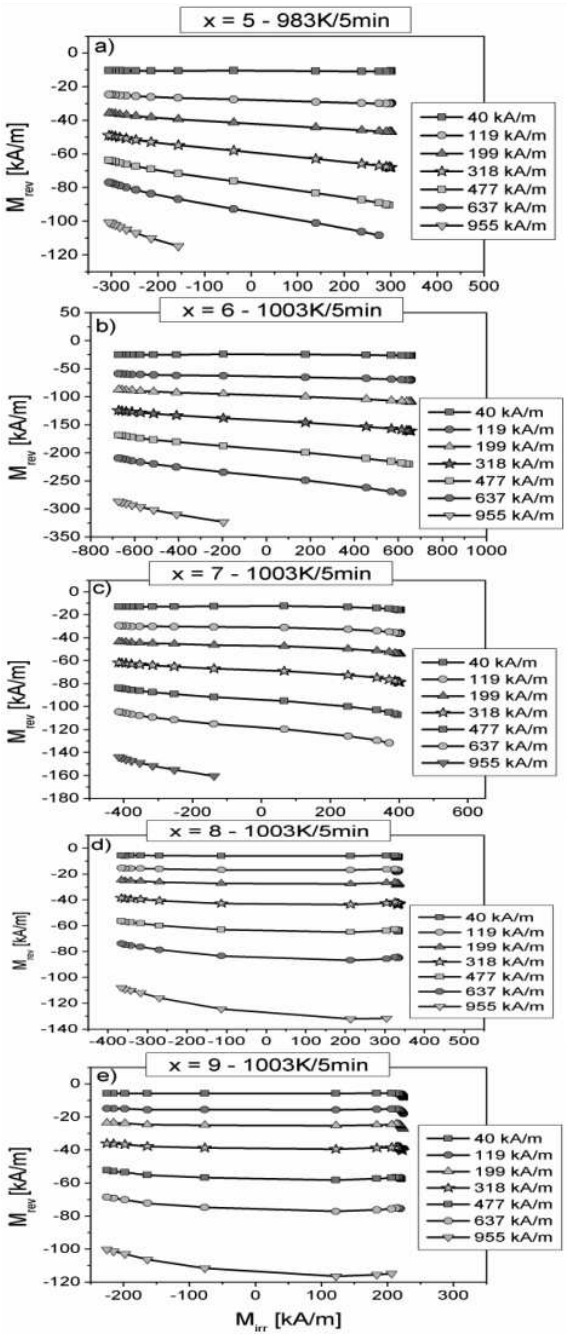

Fig. 3. The M_{rev} vs. M_{irr} dependences measured for the $(Nd_{10}Fe_{67}B_{23})_{100-x}Nb_x$, where $x = 5, 6, 7, 8, 9$ alloy ribbons annealing at 983 and 1003 K for 5 min.

ting magnetization reversal process. This confirms the results obtained from analysis of the $M_{rev}(M_{irr})$ dependences.

4. Conclusions

It was shown that the rapidly solidified $(Nd_{10}Fe_{67}B_{23})_{100-x}Nb_x$ (where $x = 5, 6, 7, 8, 9$) alloy ribbons had partial crystalline structure. The heat treatment of these ribbons at temperatures higher than 923 K led to the nucleation and growth of the hard magnetic $Nd_2Fe_{14}B$, $Nd_2Fe_{23}B_3$, and $Nd_{1+\varepsilon}Fe_4B_4$ phases. Shapes of the $M_{rev}(M_{irr})$ dependences indicate that the magnetization reversal proceeds through the nucleation of the reversal domain for ribbons doped with 5–7 at.% of Nb and a more complex reversal process for ribbons doped with 8 and 9 at.% of Nb. Here the pinning of the domain walls prevails in the nucleation of the reversed domains process. For the $x = 8$ alloy the influence of the annealing temperature on the magnetic reversal process was confirmed by the ${}_JH_C(H)$ and $J_r(H)$ measurements. For samples annealed at low temperatures (943 K), the coercivity mechanism is controlled by the nucleation and growth of the reversed domains. With the increase of the annealing temperature (above 963 K) the domain wall pinning is dominant.

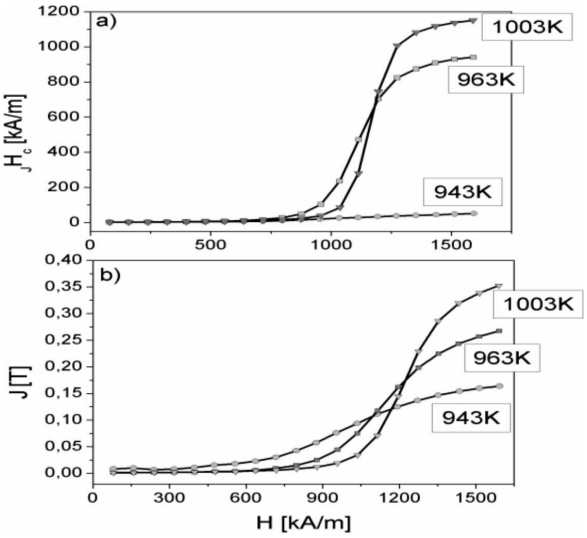

Fig. 4. ${}_JH_C$ dependences on the maximum external magnetic field H measured at initially demagnetized state (a), initial magnetization curves (b), measured for the $(Nd_{10}Fe_{67}B_{23})_{98}Nb_8$ alloy ribbons annealing at 943, 963, and 1003 K for 5 min.

References

[1] R. Skomski, J.M.D. Coey, *Permanent Magnetism*, Institute of Physics Publ., Bristol 1999.

[2] H. Zhang, Ch. Rong, X. Du, J. Zhang, S. Zhang, B. Shen, *Appl. Phys. Lett.* **82**, 4098 (2003).

[3] D.C. Crew, L.H. Lewis, D.O. Welch, F. Pourarian, *J. Appl. Phys.* 87, 4744 (2000).

[4] D.C. Crew, L.H. Lewis, *J. Appl. Phys.* 87, 4783 (2000).

[5] K. Pawlik, P. Pawlik, J.J. Wysłocki, W. Kaszuwara, *Acta Phys. Pol. A* **113**, 39 (2008).

[6] H. Kronmüller, D. Goll, *Scr. Mater.* **47**, 551 (2002).

[7] D. Givord, M.E. Rossignol, D.W. Taylor, *J. Phys. (France) IV* **2**, C3-95 (1992).

[8] D.C. Crew, P.G. McCormic, R. Street, *J. Appl. Phys.* **86**, 3278 (1999).